Topological phases, Majorana modes and quench dynamics in a spin ladder system

Wade DeGottardi,[1] Diptiman Sen,[2] and Smitha Vishveshwara[1]
[1]*Department of Physics, University of Illinois at Urbana-Champaign, 1110 W. Green St. , Urbana, IL 61801-3080, USA*
[2]*Centre for High Energy Physics, Indian Institute of Science, Bangalore 560012, India*

We explore the salient features of the 'Kitaev ladder', a two-legged ladder version of the spin-1/2 Kitaev model on a honeycomb lattice, by mapping it to a one-dimensional fermionic p-wave superconducting system. We examine the connections between spin phases and topologically non-trivial phases of non-interacting fermionic systems, demonstrating the equivalence between the spontaneous breaking of global $\mathbb{Z}_2$ symmetry in spin systems and the existence of isolated Majorana modes. In the Kitaev ladder, we investigate topological properties of the system in different sectors characterized by the presence or absence of a vortex in each plaquette of the ladder. We show that vortex patterns can yield a rich parameter space for tuning into topologically non-trivial phases. We introduce a new topological invariant which explicitly determines the presence of zero energy Majorana modes at the boundaries of such phases. Finally, we discuss dynamic quenching between topologically non-trivial phases in the Kitaev ladder, and in particular, the post-quench dynamics governed by tuning through a quantum critical point.

I. INTRODUCTION

It has been recognized recently that non-interacting fermionic lattice systems can exhibit a rich variety of phases based on their topological properties. On the other hand, it has been long known that a class of spin systems can be mapped to non-interacting fermionic systems. Here, we exploit the mapping to tailor the recent insights in fermionic systems to the context of spin systems, in particular, to a system which we dub the 'Kitaev ladder'. The Kitaev ladder is a quasi one-dimensional (1D) analog of the Kitaev model on the honeycomb lattice [1], a model which has been extensively studied for its topological aspects [2–9]; the ladder system shares many of the important features of the parent two-dimensional (2D) system. The ladder has two legs with spin-1/2 degrees of freedom at each lattice site, highly asymmetric couplings between nearest-neighbor spins, and conserved $\mathbb{Z}_2$ degrees of freedom on each plaquette associated with the presence or absence of a vortex. We will show that this ladder can be mapped to the celebrated one-dimensional p-wave superconducting system.

In pioneering work [10], Kitaev showed that a 1D p-wave superconducting system can exhibit topologically distinct phases characterized by a topological $\mathbb{Z}_2$ index. This index characterizes the topology of any one-dimensional particle-hole symmetric topological insulator [11]. Topologically non-trivial phases are characterized by the presence of localized zero energy Majorana modes at the ends of an infinitely long system having open boundary conditions; kinetic energy and superconducting pairing, so to speak, conspire to split the Dirac fermions comprising the system into their 'real' and 'imaginary' parts. Here, we discuss the manner in which these specific topological aspects and phases translate to the context of spin chains. Topologically non-trivial phases in the fermionic system may be associated with symmetry-broken phases in the spin systems, and the trivial phases with paramagnetic phases. As observed in [2, 3], we find that the presence of isolated Majorana modes at the ends of a long system with open boundary conditions is intimately related to spontaneous breaking of a global $\mathbb{Z}_2$ symmetry. We build on this observation by explicitly demonstrating the connection between spontaneous broken symmetry in a spin system and Majorana modes in the corresponding fermion system. While the behavior of spin expectation values and correlations is generally related to those of fermions in a complex, non-local fashion, the language of topology provides an immediate and novel perspective on spin phases.

The connection between topologically non-trivial and magnetic phases is generic to a large class of spin systems. What distinguishes the Kitaev ladder is the set of $\mathbb{Z}_2$ degrees of freedom associated with different vortex sectors. In the parent Kitaev honeycomb system, while most studies have focused on the ground state sector corresponding to the absence of a vortex in every plaquette, studies of other vortex sectors have been sparse. Here, the ladder system provides a simple prototype for studying the physics of different vortex sectors. The distribution of vortices on plaquettes can, in the corresponding fermionic system, be encoded in the sign of the chemical potential on each lattice site. We explore the phases realized in a range of periodic vortex sectors and find novel conditions for the existence of topologically non-trivial states. For instance, unlike in the regular 1D p-wave superconducting system, some sectors require a critical amount of superconductivity (reflected by the magnitude of the superconducting gap parameter) to host non-trivial states.

Of late, motivated by applications to topological quantum computational schemes [12], there has been a surge of interest in seeking out systems and geometries that can realize and manipulate isolated Majorana modes [3, 13–25, 27–

31]. Some analogous studies in the Kitaev honeycomb system have identified Majorana modes bound to vortices and schemes for their manipulation [15]. In the ladder system, the isolated modes, as opposed to being present at vortices, completely parallel the 1D p-wave superconducting system in being present at the interface between topologically trivial and non-trivial segments. Moreover, we find that the periodic patterns mentioned above provide a new route for finding phases and configurations that support these modes. In principle, for translationally invariant systems, such phases can be characterized by a $\mathbb{Z}_2$ topological index that considers the Berry phase accumulated by the eigenvectors in traversing the first Brillouin zone. In practice, we find that for complex periodic patterns, such a treatment proves to be rather involved, and can be replaced by the evaluation of a much more direct topological invariant derived from the equations of motion. Our method generalizes the identification of zero energy plane waves by Wen and Zee [32] to the case of evanescent modes. We use this scheme to pinpoint several different configurations of periodic patterns that yield localized Majorana modes in the bulk or at the ends of the Kitaev ladder. Our analysis also provides an alternate route for isolating Majorana modes in 1D p-wave superconductors by applying appropriate periodic potentials.

The manipulation of the Majorana modes requires dynamically changing the parameters associated with the Hamiltonian describing the system. We consider dynamics from two angles. Based on the parallel between spin and fermionic systems, we briefly outline the first steps necessary for realizing schemes in the Kitaev ladder that are analogs of those recently proposed in the 1D p-wave superconductor. Our second study of dynamics entails quenching between topologically trivial and non-trivial regions, an operation that is necessary for several dynamic schemes. The quench dynamics is interesting in its own right from the perspective of non-equilibrium quantum critical phenomena, and we find that it results in the generation of residual energy or defects whose density scales as $1/\sqrt{\tau}$ in the thermodynamic limit, where $1/\tau$ is the quench rate. This defect production, we believe, also has implications for finite sized regions and could contribute to quantum decoherence.

Our presentation is arranged as follows. In section II, we recapitulate the key features of the 1D p-wave superconductor and its topological aspects. We then show its connections to spin physics in the context of the extensively spin-1/2 XY chain subject to a transverse magnetic field. In section III, we introduce the model of interest, the Kitaev ladder, map it to the 1D p-wave superconductor and outline techniques for isolating Majorana modes in this system. In section IV, we present various vortex sectors in the Kitaev ladder system, the phases realized in these sectors, and the conditions for isolating Majorana modes. We discuss dynamical aspects in section V and, in section VI, the manner in which our studies and findings would translate back to the 1D p-wave superconductor.

II. CONNECTIONS BETWEEN 1D p-WAVE SUPERCONDUCTORS AND SPIN CHAINS

A. The 1d p-wave superconductor: recapitulation

The 1D p-wave superconducting system of spinless fermions explored by Kitaev [10] is described by the tight-binding Hamiltonian

$$H = \sum_n \left[-w\left(f_n^\dagger f_{n+1} + f_{n+1}^\dagger f_n\right) + \Delta\left(f_n f_{n+1} + f_{n+1}^\dagger f_n^\dagger\right) - \mu\left(f_n^\dagger f_n - 1/2\right)\right], \tag{1}$$

where w is the nearest-neighbor hopping amplitude, Δ the superconducting gap function (assumed real), and μ the on-site chemical potential. The translationally invariant system can be diagonalized in the momentum basis, $f_k = \frac{1}{\sqrt{N}}\sum_n f_n e^{-ikn}$ and shown to have the particle-hole symmetric dispersion

$$\omega_k \;=\; \pm\; \sqrt{(2w\cos k + \mu)^2 + 4\Delta^2 \sin^2 k}. \tag{2}$$

As shown in Fig. 1, the system hosts distinct phases depending on the parameter $|\mu|/2w$; the system is gapped save for the regions demarcating the phase boundaries. The weak (*intra*-site) pairing phase $|\mu|/2w < 1$ (phases I and II in Fig. 1) is topologically non-trivial while the strong pairing phase (phases III and IV) is topologically trivial.

Topologically trivial versus non-trivial phases are distinguished by the absence versus presence of boundary Majorana modes, which can be visualized in a simple fashion in the extreme strong and weak pairing limits as follows. Consider decomposing the Dirac f-fermion above in terms of two Majorana fermions $f_n = (a_n + ib_n)/2$, where the Majorana fermions respect the relations $a_n^2 = b_n^2 = 1$, $\{a_n, a_m\} = \{b_n, b_m\} = 2\delta_{m,n}$, $\{a_n, b_m\} = 0$. In terms of the Majorana fermions, the Hamiltonian in equation (1) becomes

$$H \;=\; \frac{i}{2}\sum_n \left[(-w+\Delta)\, a_n b_{n+1} \;+\; (w+\Delta)\, b_n a_{n+1} \;-\; \mu a_n b_n\right], \tag{3}$$

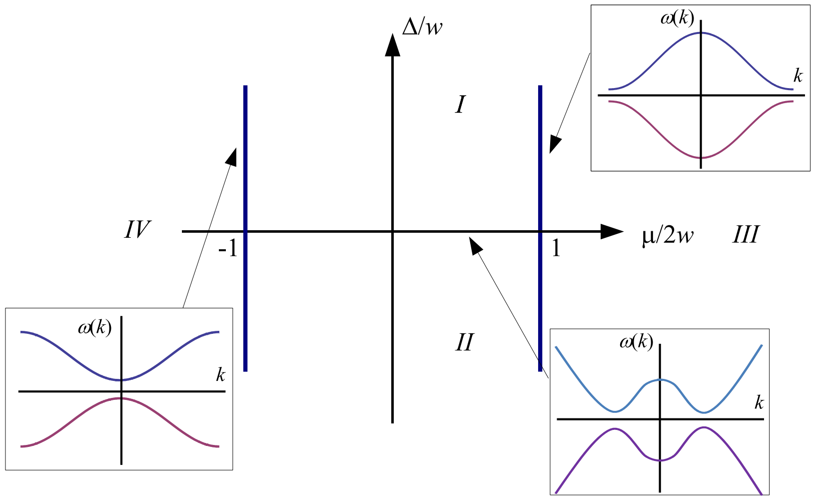

FIG. 1: Zero temperature phase diagram of the 1D p-wave superconducting fermionic system as well as the spin-1/2 XY chain in a transverse magnetic field. Phases I and II denote topologically non-trivial/ferromagnetic phases while phases III and IV denote topological trivial/paramagnetic phases. Inset: Dispersion relations near various gap closures at phase boundaries.

as represented in Fig. 2(a).

In the extreme weak pairing limit $\Delta = w > 0$, $\mu = 0$, the tight-binding Hamiltonian in (1) couples the Majorana fermions in the staggered fashion shown in Fig. 2(c). A change in sign of Δ corresponds to shifting the staggered pattern by a lattice site, thus exchanging the roles of the a and b fermions. The superconductivity induced anomalous term and the normal hopping term conspire to separate a Dirac fermion into its Majorana components, leaving an isolated Majorana mode at each end. In this limit, equation (1) decouples into the form $\sum_{n=1}^{N-1}(w+\Delta)(\tilde{f}_n^\dagger \tilde{f}_n - 1/2)$, where $\tilde{f}_n = (a_n + ib_{n+1})/2$ corresponds to Dirac fermions composed of the pairs of linked Majorana fermions depicted in Fig. 2(c). This then yields two Majorana fermions b_1 and a_N which are isolated at the two ends and which do not appear in the Hamiltonian since these modes have zero energy [10]. In the extreme strong pairing limit $\Delta = w = 0$, $\mu \neq 0$, the Majorana fermions a_n and b_n are pairwise connected as shown in Fig. 2(b); thus no Majorana fermions are isolated.

The presence of an energy gap in each phase ensures that slightly changing the couplings from these extreme limits does not alter these topological aspects. In the weak pairing phase, it is thus still possible to define appropriate linear combinations $Q_L = \sum \alpha_n a_n$ and $Q_R = \sum \beta_n b_n$ (with α_n and β_n real) that are Majorana modes bound to the two ends of the system and that become isolated in the thermodynamic limit.

B. Mapping spin chains to a p-wave superconductor

The concepts discussed above can be investigated in the context of spin chain physics. As an example, consider the extensively studied spin-1/2 XY chain subject to a transverse magnetic field [33–35]. The Hamiltonian is given by

$$H = -\sum_{n=1}^{N-1} \left(J_x \sigma_n^x \sigma_{n+1}^x + J_y \sigma_n^y \sigma_{n+1}^y\right) - h\sum_{n=1}^{N} \sigma_n^z, \tag{4}$$

where σ_n^α denote the Pauli matrices. The spin-1/2 operators can be mapped to Majorana fermions using the Jordan-Wigner transformation [33, 36] $a_n = \prod_{j=1}^{n-1} \sigma_j^z \ \sigma_n^x, b_n = \prod_{j=1}^{n-1} \sigma_j^z \ \sigma_n^y$, for $2 \leq n \leq N$, $a_1 = \sigma_1^x$ and $b_1 = \sigma_1^y$. The resultant Hamiltonian exactly maps to the 1D p-wave superconductor Majorana Hamiltonian of equation (3) with the identification $w \leftrightarrow J_x + J_y$, $\Delta \leftrightarrow J_y - J_x$, $\mu \leftrightarrow 2h$, and with the interchange of a_n and b_n on even sites. Hence, Fig. 1 also represents the phase diagram for the spin system. Phases I and II are ferromagnetic and have non-zero ground state expectation values of σ_n^x and σ_n^y, respectively. Phases III and IV are paramagnetic with both σ_n^x and σ_n^y having zero expectation values in the ground state. The extreme limits shown in Fig. 2 can be understood in terms of spin physics. The case of Fig. 2(c) corresponds to the values of the couplings $J_x \neq 0, J_y = 0, h = 0$ and thus to an Ising-type ferromagnetic (or antiferromagnetic) ground state along the x-axis. The case of Fig. 2(b) corresponds to $J_x = 0, J_y = 0, h \neq 0$ and thus to spins polarized along the z direction.

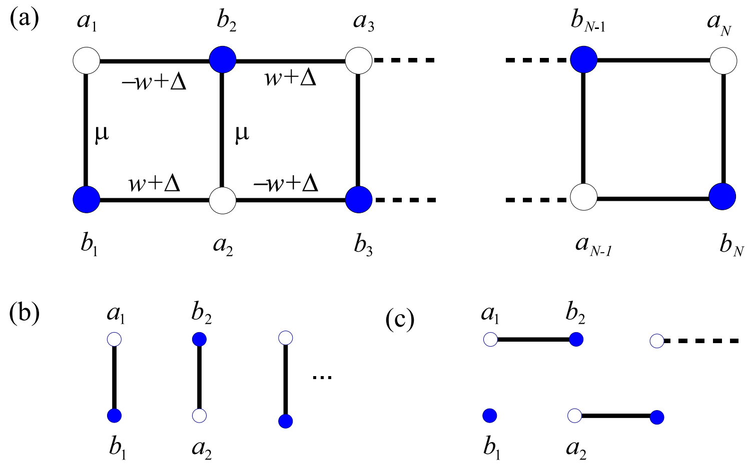

FIG. 2: Pictorial representation of the couplings between Majorana fermions described by the Hamiltonian in equation (3) for the cases of (a) general couplings, (b) the strong (intra-site) pairing limit $\Delta = w = 0$, $\mu \neq 0$ which does not possess Majorana modes (topologically trivial), and (c) the weak pairing limit $\Delta = -w$, $\mu = 0$ which hosts Majorana modes at the ends (topologically non-trivial).

C. Spontaneous symmetry breaking and isolated Majorana modes

As discussed above, the topologically non-trivial phases in the p-wave superconductor, associated with isolated boundary Majorana fermions, map onto the ferromagnetic phases in the spin chain. We argue here as follows that the presence of these isolated fermions corresponds to a $\mathbb{Z}_2$ symmetry in the spin phases which gets broken spontaneously. As is obvious in the extreme limit of Fig. 2(c), the energetics in phases I and II provides $N-1$ constraints for a system of N spins. Hence, the ground state is constrained to two degenerate states reflecting a $\mathbb{Z}_2$ symmetry. Returning to the language of fermions, the degeneracy is associated with the isolated modes $Q_L = \sum \alpha_n a_n$ and $Q_R = \sum \beta_n b_n$ which do not participate in the energetics. Explicitly, the Dirac fermion formed by the two boundary Majorana fermions, $\Psi = (Q_L + iQ_R)/2$ can have occupation number 0 or 1. Thus, picking one of the corresponding degenerate states $|0\rangle_\Psi$ or $|1\rangle_\Psi$ (or any linear combination $u|0\rangle_\Psi + v|1\rangle_\Psi$) amounts to breaking the $\mathbb{Z}_2$ symmetry of the ground state and picking one of the two energetically available spin configurations. In phases III and IV, however, energetics poses N constraints and the system is confined to a unique ground state.

To explore the spin physics in the symmetry broken phase in terms of the isolated Majorana modes, consider the spin-1/2 algebra formed by $\{Q_L, Q_R, -iQ_LQ_R\}$, where $iQ_LQ_R = 2\Psi^\dagger\Psi - 1$. The two eigenstates of any of these operators (those of the $-iQ_LQ_R$ being $|0\rangle_\Psi$ and $|1\rangle_\Psi$) are orthogonal to one another and are each equally valid configurations in the ground state. The particular symmetry broken choice immediately determines the expectation values of these operators and their corresponding Majorana and spin operators. Specifically, if we consider the two eigenstates of Q_L, $|\psi_\pm\rangle_L$, we can use the relationship $\{Q, a_n\} = 2\alpha_n$ to show that $\langle\psi_+|a_n|\psi_+\rangle_L = \alpha_n$ and $\langle\psi_-|a_n|\psi_-\rangle_L = -\alpha_n$ for all n. Furthermore, since $\{Q, b_n\} = 0$, we see that $\langle\psi_\pm|b_n|\psi_\pm\rangle_L = 0$ for all n. The physics behind these statements can be made more transparent, for instance, in the limiting case $J_x > |J_y|$ and $h = 0$. Here, the system is in the Ising-type phase whose possible degenerate ground states correspond to spins that are either primarily aligned or anti-aligned along the $\hat{x}$ direction. In fact, $|\psi_\pm\rangle_L$ are exactly these two states. Given that σ_1^x is identically a_1, we can easily evaluate its expectation value in one of the states to get $\langle\psi_+|\sigma_1^x|\psi_+\rangle_L = \sqrt{1-(J_y/J_x)^2}$, as ought to be true for the system pointing primarily along $\hat{x}$.

The non-local nature of the Majorana modes is consistent with the spontaneously broken symmetry being global. Energetics locks all spins into one of two possible configurations where the Jordan-Wigner string connects the chain in a non-local, highly entangled fashion. A particular choice of states in the basis of the isolated Majorana modes thus corresponds to picking one of these highly entangled states. It should be noted that a knowledge of which one of these states is chosen, for instance $|\psi_+\rangle_L$, gives limited information in that expectation values can be evaluated only for non-local spin operators corresponding to Majorana modes a_n and b_n, except for one or two operators, such as σ_1^x above. This knowledge does provide evidence for long-range order. For example, our result for $\langle\psi_+|\sigma_1^x|\psi_+\rangle_L$ in the example above can be compared to that of Lieb, Schultz and Mattis [33]. It is shown in Ref. [33] that, for an open chain with N sites (where N is even and $\to \infty$) in a case which is effectively that of the Ising limit above, the end-to-end two-point correlation functions are given by $\langle\psi_+|\sigma_1^x\sigma_N^x|\psi_+\rangle = 1-(J_y/J_x)^2$ and $\langle\psi_+|\sigma_1^y\sigma_N^y|\psi_+\rangle = 0$. In the

limit $N \to \infty$, we expect clustering to hold, so that $|\langle\psi_+|\sigma_1^x|\psi_+\rangle| = |\langle\psi_+|\sigma_1^x\sigma_N^x|\psi_+\rangle|^{1/2}$. We therefore find complete agreement with the results in [33]. We note that our derivation is much simpler than the one in Ref. [33], purely making use of the end Majorana modes, and our results can be easily generalized to take into account the transverse magnetic field h in Eq. (4) which was not considered in [33]. Thus, analysis of the isolated Majorana modes can be a valuable means for gaining insight into spin chain physics.

III. THE KITAEV LADDER SYSTEM

A. The model

Equipped with the connection between a 1D p-wave superconductor and spin chains, we turn to the object of our attention, the Kitaev ladder system. This system consists of a single (modified) strip of Kitaev's original two-dimensional honeycomb system. The model is thus ladder-like and each plaquette is a square instead of a hexagon. As shown in Fig. 3, the two-legged ladder hosts spin-1/2 degrees of freedom at sites (n, u) and (n, l), where u, l denote the upper and lower legs, respectively. The Hamiltonian is given by

$$\begin{aligned} H &= \sum_{n=1}^{(N-1)/2} \left[J_x\left(\sigma^x_{2n-1,u}\sigma^x_{2n,u} + \sigma^x_{2n,l}\sigma^x_{2n+1,l}\right)\right. \\ &\left. + J_y\left(\sigma^y_{2n,u}\sigma^y_{2n+1,u} + \sigma^y_{2n-1,l}\sigma^y_{2n,l}\right)\right] + \sum_{n=1}^{N} J_z\sigma^z_{n,u}\sigma^z_{n,l}, \end{aligned} \tag{5}$$

where $\sigma^i_{n,u/l}$ denote the Pauli matrices respecting the usual commutation rules, $\left[\sigma^i_{n,s}\sigma^j_{m,s'}\right] = 2i\delta_{m,n}\delta_{s,s'}\epsilon_{ijk}\sigma^k_{n,s}$.

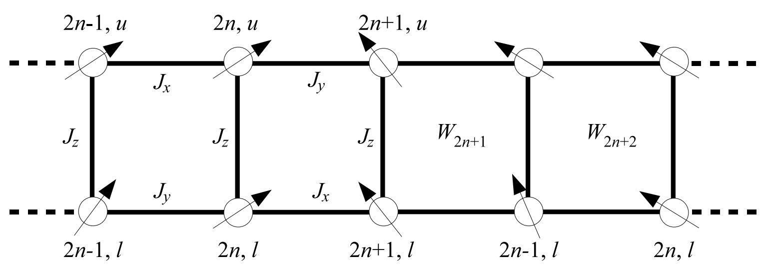

FIG. 3: The Kitaev ladder, the associated couplings J_x, J_y and J_z, and the vortex operators, W_n.

As in the 2D honeycomb lattice system, each plaquette has an associated operator W_n which commutes with the Hamiltonian and is of the form $\sigma^x_{n,u}\sigma^x_{n+1,u}\sigma^y_{n+1,l}\sigma^y_{n+1,l}$ for n even and $\sigma^y_{n,u}\sigma^y_{n+1,u}\sigma^x_{n,l}\sigma^x_{n+1,l}$ for n odd. Since $W_n^2 = 1$, the eigenvalues of W_n are ± 1; hence these invariants provide a set of $\mathbb{Z}_2$ quantum numbers characterizing different sectors of the Hamiltonian. These operators, commonly referred to as vortex operators, reflect the absence/presence ($W_n = \pm 1$) of a vortex in each plaquette. The richness of this system, its phases and its topological properties derive from the extensive space of the $\mathbb{Z}_2$ configurations.

B. Jordan-Wigner transformation

The Kitaev ladder/honeycomb system is endowed with a special set of couplings which enable the Jordan-Wigner transformation to provide a *local* fermionic Hamiltonian [2, 7]. As in the previous section, this transformation gives a direct connection between the Kitaev ladder and the 1D p-wave superconductor. The mapping relates spin operators to Majorana fermionic operators:

$$\begin{aligned} a_n &= S_{n,l/u}\sigma^{x/y}_{n,l/u}, \quad b_n = \pm S_{n,u/l}\sigma^{x/y}_{n,u/l}, \quad \text{for } n \text{ odd/even}, \\ c_n &= S_{n,l/u}\sigma^{y/x}_{n,l/u}, \quad d_n = \pm S_{n,u/l}\sigma^{y/x}_{n,u/l}, \quad \text{for } n \text{ odd/even}. \end{aligned} \tag{6}$$

Here, assuming that each leg contains N sites with open (rather than periodic) boundary conditions, the string operator $S_{n,u} = \prod_{m=1}^{n-1} \sigma^z_{m,u}$ runs from the left to the right along the top leg in Fig. 3 to the $(n-1)$-th site, while

$S_{n,l} = \prod_{m=1}^{N} \sigma^z_{m,u} \prod_{m=n+1}^{N} \sigma^z_{m,l}$ runs completely along the top leg left to right and then back along the bottom leg to the $(n+1)$-th site.

In terms of these Majorana operators, the Hamiltonian is of the form $H = \sum_n (-iJ_x a_n b_{n+1} + iJ_y b_n a_{n+1} - J_z a_n b_n c_n d_n)$. The role of the vortices is encoded in the J_z term. This can be seen by noting that $W_n = -(ic_n d_n)(ic_{n+1}d_{n+1})$ and defining $s_n = ic_n d_n = \prod_{m=n}^{N} W_m c_N d_N$. Then, the Hamiltonian, as depicted pictorially in Fig. 3, takes the form

$$H = i\sum_n (-J_x a_n b_{n+1} + J_y b_n a_{n+1} + J_z s_n a_n b_n), \tag{7}$$

where $s_n = \pm 1$ depending on the configuration of vortices, namely $W_n = -s_n s_{n+1}$. Now, to make a connection with the p-wave system, one can once more define Dirac fermions $f_n = (a_n + ib_n)/2$ as in the XY spin chain. The vorticity can be captured by another set of Dirac fermions, $g_n = (c_n + id_n)/2$; s_n, which we coin 'site-polarity', reflects the occupancy of these fermions via $s_n = 2g_n^\dagger g_n - 1$ and determines the sign of the chemical potential for the f-fermions

In terms of the Dirac fermions, the Kitaev ladder also maps onto the 1D p-wave superconductor form,

$$\begin{aligned} H = \; - \; & \sum_n [w\left(f_n^\dagger f_{n+1} + f_{n+1}^\dagger f_n\right) \\ & - \; \Delta\left(f_n f_{n+1} + f_{n+1}^\dagger f_n^\dagger\right) \; - \; \mu_n\left(f_n^\dagger f_n - 1/2\right)], \end{aligned} \tag{8}$$

where the identification

$$w \leftrightarrow J_x + J_y, \quad \Delta \leftrightarrow J_y - J_x, \quad \text{and} \quad \mu_n \leftrightarrow 2 s_n J_z \tag{9}$$

has been made. Thus, the f-fermions, as in the XY spin chain, participate in the dynamics, while the g-fermions encode the vortex configurations. Each set of fermions spans a Hilbert space of size 2^N, together comprising the Hilbert space of size 2^{2N} thus accounting for all the degrees of freedom of the original $2N$ spins of the ladder system.

Compared to the XY spin chain of the previous section, one main difference in the mapping to the p-wave superconductor is that the sign of the chemical potential is position dependent. Here, we restrict our studies to periodic patterns. For s_n with period p, we can employ the decomposition

$$s_n \; = \; \sum_{q=0}^{p-1}\left(s_q e^{i2\pi qn/p} \; + \; s_q^* e^{-i2\pi qn/p}\right). \tag{10}$$

In the momentum basis ($f_k = \frac{1}{\sqrt{N}}\sum_n f_n e^{-ikn}$), the Dirac Hamiltonian describing the Kitaev ladder then takes the form (up to an overall constant)

$$\begin{aligned} H \; = \; & \sum_{0\le k<\pi}\left[-2w\cos k\left(f_k^\dagger f_k + f_{-k}^\dagger f_{-k}\right) + \Delta\left(e^{ik} f_k^\dagger f_{-k}^\dagger + e^{-ik} f_{-k} f_k\right)\right] \\ & -2J_z \sum_{0\le k<2\pi}\sum_{q=0}^{p-1}\left(s_q f_{k+2\pi q/p}^\dagger f_k + s_q^* f_{k-2\pi q/p}^\dagger f_k\right). \end{aligned} \tag{11}$$

The other difference between the ladder and the XY spin chain is in the degrees of freedom. Here, the ladder Hamiltonian provides $N-1$ constraints on the energetics for a ladder of $2N$ spins. An additional $N-1$ constraints are given by the configuration of vortices (note that another $\mathbb{Z}_2$ symmetry is present because the vortex eigenvalues of W_n are invariant under a global sign change of the s_n's). These constraints together connect all $2N$ spins. Hence, once again the topologically non-trivial phases, namely those bearing isolated boundary Majorana modes, can be associated with spontaneous symmetry breaking in the spin language; a detailed study of the spin physics, as initiated for the XY spin chain, is in order.

C. Techniques for identifying isolated Majorana modes

The fermionic Hamiltonian in Eq. (8) provides a starting point for exploring various conditions under which bulk or boundary Majorana modes may appear. In this section, we develop a formalism which enables us to identify these modes in a range of vortex sectors. We avail ourselves of the transfer matrix method which has been used extensively in 1D systems [37, 38] and is well suited to study bound states. The presence of bound Majorana states is governed by the growth or decay of the eigenfunctions of the transfer matrix. As a way of discerning the existence of these states, we employ an invariant which is constructed by analytically continuing plane wave states.

1. Transfer matrix approach

The transfer matrix can be constructed by employing the Heisenberg representation and deriving the equations of motion from the Hamiltonian of Eq. (7) for the time dependent Majorana modes $a_n = \alpha_n e^{-i\omega t}$ and $b_n = \beta_n e^{-i\omega t}$. These equations are of the form

$$\begin{aligned} (w-\Delta)\,\alpha_{n-1} + (w+\Delta)\,\alpha_{n+1} - \mu_n\alpha_n &= -i\omega\beta_n, \\ -(w+\Delta)\,\beta_{n-1} - (w-\Delta)\,\beta_{n+1} + \mu_n\beta_n &= -i\omega\alpha_n, \end{aligned} \tag{12}$$

where we have invoked the identification in Eq. (9).

To identify Majorana modes, we focus on $\omega = 0$ corresponding to real values of α_n and β_n. The equations for α_n and β_n decouple, and they can be written in the transfer matrix form

$$\begin{pmatrix} \alpha_{n+1} \\ \alpha_n \end{pmatrix} = A_n \begin{pmatrix} \alpha_n \\ \alpha_{n-1} \end{pmatrix}, \quad \text{where} \quad A_n = \begin{pmatrix} \frac{\mu_n}{\Delta+w} & \frac{\Delta-w}{\Delta+w} \\ 1 & 0 \end{pmatrix}. \tag{13}$$

Similar expressions hold for the β_n's since the respective transfer matrices are related by $B_n = A_n^{-1}$. Knowing the behavior of the a-modes thus completely determines that of the b-modes.

This transfer matrix formulation enables us to study the growth versus decay of modes at the boundary of a finite piece of the ladder or at the interface between two parts of the ladder in different phases. In particular, for a homogeneous system having all couplings and s_n constant, this behavior is determined by the eigenvalues of any A_n, while for a region having periodicity p in the s_n's, it is determined by the eigenvalues of the matrix

$$\mathcal{A}_P = A_p\, A_{p-1}\, \cdots\, A_2\, A_1. \tag{14}$$

Majorana modes bound to the ends of a finite chain require that both eigenvalues of $\mathcal{A}_P$ be either smaller or greater than unity in magnitude. The former case corresponds to an a-mode localized at the left end and a b-mode at the right end. The conditions on the eigenvalues ensure that the localized modes can simultaneously respect constraints at the boundary and normalizability. For instance, if the chain goes from $n = 1$ to ∞, the condition to be imposed on the Majorana mode at the left end is that $\alpha_0 = 0$ and $\alpha_1 = c$, where c is a non-zero constant to be fixed by the normalization. The corresponding vector $\begin{pmatrix} \alpha_1 \\ \alpha_0 \end{pmatrix} = \begin{pmatrix} c \\ 0 \end{pmatrix}$ can be written as a linear superposition of the two eigenvectors of $\mathcal{A}_P$. We then see from Eq. (13) that $\alpha_n \to 0$ as $n \to \infty$ if both the eigenvalues of $\mathcal{A}_P$ are smaller than unity.

Bound Majorana states in the bulk of the chain can be realized by juxtaposing two regions corresponding to different phases. The highlighting feature of this system is its ability to dial in to different phases by changing the vortex patterns. We thus consider the interface of two semi-infinite patterns P $(n < 0)$ and Q $(n \geq 0)$ having periodicities p and q, respectively, but with the same values of the couplings w, Δ, and μ. Considerations similar to those above enable us to identify two situations in which there exists exactly one normalizable Majorana mode for n tending to both ∞ and $-\infty$. These correspond to (i) $\mathcal{A}_P$ having both eigenvalues larger than 1 in magnitude or both smaller than 1 and $\mathcal{A}_Q$ having exactly one eigenvalue less than 1 in magnitude, or (ii) $\mathcal{A}_P$ having exactly one eigenvalue larger than 1 in magnitude and $\mathcal{A}_Q$ having both eigenvalues less than 1 or both smaller than 1 in magnitude. Other situations yield either no bound mode or a pair of concurrent Majorana modes.

2. Topological invariant

The relevant features of the transfer matrix structure can be gleaned by a simple consideration of its analytic properties. This analysis extends the application of the topological invariant introduced by Wen and Zee [32] to the study of evanescent modes. Our construction of the invariant is derived from $f(z)$, the characteristic polynomial of $\mathcal{A}_P$. Given that $\mathcal{A}_P$ is a real 2×2 matrix, a single root inside the unit disk must lie on the real axis. Thus the index

$$\nu = -\ \operatorname{sgn}\left(f(1)f(-1)\right), \quad \text{where} \quad f(z) = \det(\mathcal{A}_P - Iz), \tag{15}$$

is equal to 1 if and only if $\mathcal{A}_P$ has exactly one eigenvalue with a magnitude less than 1. This case of $\nu = 1$ indicates a topologically trivial state, i.e., one with no end Majorana modes. However, $\nu = -1$ indicates the existence of end Majorana modes reflected by $\mathcal{A}_P$ having both eigenvalues less than or both greater than 1 in magnitude. The marginal case $\nu = 0$ would imply a closure of the bulk gap. In fact, ν can only change sign if a bulk gap closes.

The invariant ν is topological in that it is derived by invoking the continuity of $f(z)$ to infer its behavior inside the unit disk based on its values on the unit circle. We believe that this index, derived using physically transparent methods, can be reduced to Kitaev's invariant based on the Pfaffian when generalized to our ladder model. The invariant ν can be related to that of Wen and Zee [32] by noting the form $\nu = (-1)^{n_f+1}$, where n_f is the number of zeros of $f(z)$ for which $|z| < 1$; in Ref. [32], the equivalence $n_f = \frac{1}{2\pi i}\oint_{|z|=1} dz\ f'(z)/f(z)$ was used to identify plane wave zero modes. Furthermore, $f(z)$ was replaced by the dispersion which can also be done in our case but makes the analysis more involved. Finally, the invariant ν can be related to the topological invariant of [11] in that they both locate zero modes but the former bypasses the need to identify the eigenvectors of Eq. (11) and the Berry phase across the Brillouin zone.

IV. VORTEX SECTORS AND ISOLATED MAJORANA MODES

We employ the transfer matrix approach and the invariant ν to show that a diverse set of patterns in the site-polarities s_n, or equivalently, vortex sectors, can host isolated Majorana modes. We focus on three classes of vortex sectors (i) the full vortex sector defined by $s_n = 1$, (ii) the zero vortex sector defined by $s_n = (-1)^n$, and which is associated with the ground state sector in the parent 2D model, and (iii) patterns of s_n having higher periodicity.

A. Full vortex sector: $s_n = 1$

The full vortex sector maps directly to the XY spin chain in the transverse field as well as the homogeneous 1D p-wave superconductor. Isolated Majorana modes have been well-studied in the latter case and are expected to exist at the ends of wires in the topologically non-trivial phases I and II in Fig. 1 and at the boundary between a topologically non-trivial phase and topologically trivial phase in the phase diagram of Fig. 1. We expand on these arguments to illustrate the techniques developed here and to provide a comprehensive description of the Kitaev ladder. In the next subsection, we also show that this sector corresponds to the ground state sector in a certain parameter range.

1. End modes

The condition for Majorana modes to exist at the ends of the Kitaev ladder is given by $\nu = -1$, where ν is the topological invariant of equation (15). For the full vortex sector, we have a uniform site-polarity, $s_n = 1$ for all n; the corresponding site-independent transfer matrix is given by

$$\mathcal{A} = \begin{pmatrix} \frac{\mu}{\Delta+w} & \frac{\Delta-w}{\Delta+w} \\ 1 & 0 \end{pmatrix}, \tag{16}$$

which yields

$$f(z) \ = \ \det(\mathcal{A} - Iz) \ = \ z^2 - \left(\frac{\mu}{\Delta+w}\right) z \ - \ \left(\frac{\Delta-w}{\Delta+w}\right). \tag{17}$$

Hence,

$$\nu \ = \ - \ \mathrm{sgn}\left(f(1)f(-1)\right) \ = \ \mathrm{sgn}\left(|\mu| - 2\,|w|\right), \tag{18}$$

for $\Delta + w \neq 0$. A consideration of the location of the zeros of $f(z)$ shows that an a (b) Majorana mode is localized to the right (left) side of the system if $2w > |\mu|$ and $\Delta > 0$. If $2w < -|\mu|$ the positions of the a and b Majoranas are switched. Switching the sign of Δ also interchanges the Majorana modes (see Fig. 4).

2. Interface modes

As an illustrative example, consider the bound modes obtained by juxtaposing two regions in phases I and III on the left and right, respectively, in the phase diagram of Fig. 1. The bound state structure at the interface can be derived by considering the closing of the gap at the phase boundary. Close to this region, the dispersion in equation (2) takes the form $\omega_k = \pm 2\sqrt{\Delta^2(\delta k)^2 + m^2}$ at $k \approx \pi$, where $m(x) = \mu/2 - w$. Here, the continuum version of the equations

of motion, equation (12), is given by $\partial_x a(x) = m(x)a(x)$ and $\partial_x b(x) = -m(x)b(x)$. In this case, the Majorana mode that satisfies normalizability takes the form $b(x) \propto e^{-\int_0^x dx' m(x')}$. In fact, this solution corresponds to that of the celebrated Jackiw and Rebbi model [39] as applied to Majorana fermions. The instances of a single bound Majorana mode at an interface are exhausted by the cases involving the juxtaposition of phases I/II ($|\mu| < 2|w|$) and phases III/IV ($|\mu| > 2|w|$). In terms of the invariant form in Eq. (17), these cases correspond to juxtaposing a topologically non-trivial ($\nu = -1$) phase with a topologically trivial phase ($\nu = 1$).

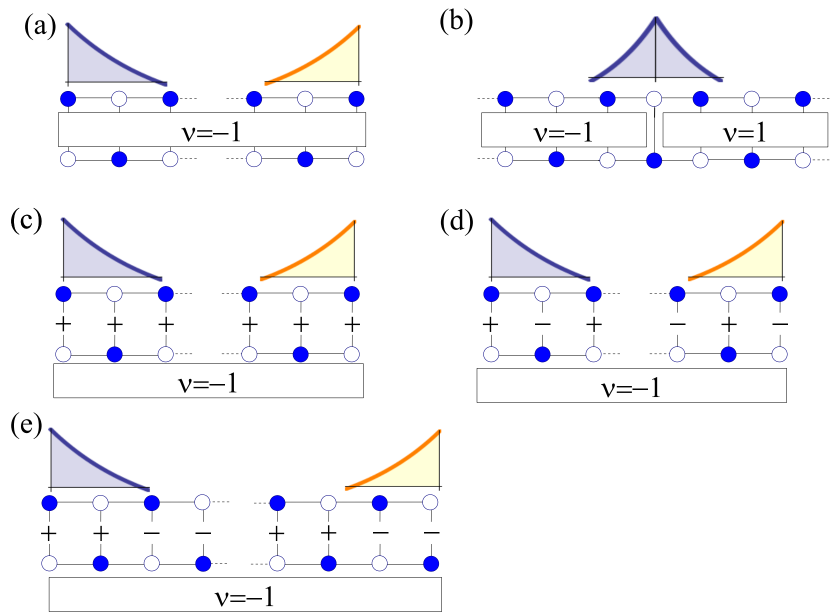

FIG. 4: Examples of isolated Majorana modes for the Kitaev ladder system. Generically, Majorana modes are hosted at (a) the ends of ladders with nontrivial topology ($\nu = -1$) or at (b) the interface between regions with $\nu = -1$ and $\nu = 1$. In the case of the uniform sector $s_n = 1$ with $2|w| > |\mu|$, individual Majorana modes are hosted at (c) each end of a ladder. Other examples of end Majorana modes include (d) the alternating sector $s_n = (-1)^n$ with $2|\Delta| > |\mu|$ and (e) the sector $P = ++--$ with $2\sqrt{|w\Delta|} > |\mu|$.

B. Vortex-free sector: $s_n = (-1)^n$

In the 2D honeycomb system, the vortex-free sector is special in that it corresponds to the ground state sector for all values of spin couplings. This condition, however, holds only for a range of parameters in the Kitaev ladder. To elucidate this, consider the limit of J_z large compared to J_x and J_y. In the language of a p-wave superconductor, let us assume that μ is large and positive. We then find that the perturbative change in the ground state energy compared to the $w = \Delta = 0$ limit is given by the second order expression

$$\Delta E_0 \;=\; -\,\frac{1}{2\mu}\sum_n \left[w^2(1 - s_n s_{n+1}) \;+\; \Delta^2(1 + s_n s_{n+1})\right]. \tag{19}$$

If $w^2 > \Delta^2$, the ground state energy is lowest if $s_n s_{n+1} = -1$ for all n, i.e., if $s_n = (-1)^n$; this is the sector with no vortices. If $w^2 < \Delta^2$, however, the ground state energy is lowest if $s_n s_{n+1} = 1$ for all n, i.e., if $s_n = \pm 1$ for all n; this is the full vortex sector. Another difference is that unlike in the 2D system, reduced dimensionality renders the Kitaev ladder system to be gapped everywhere except along phase boundaries.

For the vortex free sector, we can identify the range of parameter space which yields topologically non-trivial phases. Towards this end, we identify the period 2 transfer matrix

$$\mathcal{A} = \begin{pmatrix} -\frac{\mu}{\Delta+w} & \frac{\Delta-w}{\Delta+w} \\ 1 & 0 \end{pmatrix}\begin{pmatrix} \frac{\mu}{\Delta+w} & \frac{\Delta-w}{\Delta+w} \\ 1 & 0 \end{pmatrix}, \tag{20}$$

and the characteristic polynomial

$$f(z) = \det(\mathcal{A} - Iz) = z^2 + \left(\frac{2w^2 - 2\Delta^2 + \mu^2}{(w+\Delta)^2}\right) z + \left(\frac{\Delta - w}{\Delta + w}\right)^2 . \tag{21}$$

Our topological invariant (for $w + \Delta \neq 0$) takes the form

$$\nu \;=\; -\;\mathrm{sgn}\left(f(1)f(-1)\right) \;=\; \mathrm{sgn}\left(|\mu| - 2\,|\Delta|\right). \tag{22}$$

In this case, the topological nature of the phase depends on the relative magnitude of the superconducting order parameter and the chemical potential, as opposed to the hopping integral and the chemical potential as in the uniform case, cf. Eq. (18) and Eq. (22). That the point separating the topologically trivial and non-trivial regions derived from $\nu = 0$ is equivalent to gap closure can be gleaned from the dispersion for $s_n = (-1)^n$,

$$\omega_k^2 \;=\; 2\,\left[w^2 \;+\; \Delta^2 \;+\; \frac{\mu^2}{2} \;+\; \left(w^2 \;-\; \Delta^2\right)\cos(2k) \;\pm\; \Delta\mu\sin k\right]. \tag{23}$$

Specifically, consistent with Eq. (22), the gap closes at $k = \pm\pi/2$ for $2|\Delta| = |\mu|$. Once again, as in the full vortex sector, the isolated Majorana modes at the end of a finite chain or at the interface of two regions can be identified using Eq. 22 (see Fig. 4e). Thus we see that the imposition of a periodic pattern can give rise to qualitatively different physics in that here the topological nature of the system depends on the magnitude of Δ.

C. Higher period sectors

The consideration of periodic patterns in the site-polarity s_n's provides a zoo of configurations for realizing topologically non-trivial phases and interface Majorana modes. We can once again invoke the topological invariant ν for any periodic structure P characterized by the transfer matrix $\mathcal{A}_P$ of Eq. (14). In general, we have

$$\begin{aligned}\nu_P \;&=\; -\prod_{m=\pm}\mathrm{sgn}\left(\det\mathcal{A}_P + 1 + m\mathrm{Tr}\mathcal{A}_P\right)\\ &=\; \mathrm{sgn}\left(|\mathrm{Tr}\mathcal{A}_P| - |\det\mathcal{A}_P + 1|\right).\end{aligned} \tag{24}$$

It follows from these expressions that any two chains which are cyclic permutations of each other must have the same topology, as we would expect physically. It is also true that the transformation $s_n \to -s_n$ for all n will not change the topology of the chain. Although giving a full analytic expression is not practical, it may be noted that the detailed features of a pattern of the site polarities s_n that control its topology enter Eq. (24) through the quantity $\mathrm{Tr}\mathcal{A}_P$. Some insight can therefore be gained by an expansion in certain limits. For example, if $|\mu| < 2|w \pm \Delta|$, a useful expansion of $\mathrm{Tr}\mathcal{A}_P$ in powers of $\mu^2/(w^2 - \Delta^2)$ is (for p even)

$$\mathrm{Tr}\mathcal{A}_P = \left(\frac{\Delta - w}{\Delta + w}\right)^{p/2}\left[2 + \frac{\mu^2}{2(w^2 - \Delta^2)}\left(\sum_{m=1}^{p/2} s_{2m}\right)\left(\sum_{n=1}^{p/2} s_{2n-1}\right) + \mathcal{O}\left(\mu^4\right)\right]. \tag{25}$$

Thus, in this case the quantity $\left(\sum_{m=1}^{p/2} s_{2m}\right)\left(\sum_{n=1}^{p/2} s_{2n-1}\right)$ represents the most relevant feature of P in determining its topology. As a specific example, taking $\mathcal{A}_P = A_1A_2A_3A_4$ for a generic period 4 pattern (s_1, s_2, s_3, s_4), we get an expression for ν which is a function of $(s_1 + s_3)(s_2 + s_4)$, $s_1s_2s_3s_4$, and the couplings constants w, Δ, and μ. Thus from the standpoint of topologically non-trivial phases, there are two distinct period 4 patterns, namely $+++-$ and $++--$. For instance, the application of equation (24) to the pattern $P = ++--$ yields

$$\nu_P \;=\; \mathrm{sgn}\left(\mu^2 - 4|w\Delta|\right), \tag{26}$$

as illustrated in Fig. 4f. Similar constraints are also obtained for the other patterns, demonstrating that patterns of higher periodicity can have phase boundaries involving more intricate dependencies on the values of μ, w, and Δ. Thus, we have shown that the topology and existence of isolated Majorana modes can be controlled by configurations of vortices in the Kitaev spin ladder.

V. DYNAMICS

Having charted out the topologically non-trivial phases and associated Majorana physics in the Kitaev ladder, we move on to dynamically tuning between topologically trivial and non-trivial regions. We briefly visit this issue in the context of manipulating isolated Majorana modes and then present a comprehensive study on dynamic quenching between these regions.

A. Majorana manipulation

From the point of view of topological quantum computation, a system hosting zero energy Majorana modes can in principle store non-local quantum information. In 2D systems, gate operations on the degenerate subspace can be achieved by the dynamic interchange of such modes, exploiting the non-Abelian nature of such exchanges. Recent proposals have explored schemes for transporting isolated Majorana fermions in 1D p-wave superconductor wires and also braiding them in a network of quantum wires including T-junctions [16, 19]. These protocols are based on the tunability of the bulk topology and the controlled growth or contraction of regions of non-trivial topology.

The Kitaev ladder is well-suited to such a scheme given the many different ways of controlling the topology of the system. Primarily, moving an isolated Majorana mode would amount to dynamically moving the interface between topologically trivial and non-trivial regions, such as those shown in Fig. 4. One method of doing so would be to dynamically change the spatial profile of the couplings J_x, J_y, and J_z which determine the phases in the different regions, for instance, as shown in the phase diagram of Fig. 1. Alternatively, Majorana modes may be manipulated by changing the vortex patterns which, as discussed in section IV, determine the topology of a region. The presence or absence of a vortex is determined by the site-polarity s_n, or, equivalently, the g-fermion occupation number discussed in section III B. These occupation numbers can be controlled by a combination of operators which do not appear in the Kitaev ladder Hamiltonian in equation (5). Examples include $J_1(\sigma^y_{2n,u}\sigma^y_{2n+1,u} - \sigma^x_{2n,l}\sigma^x_{2n+1,l}) = 2iJ_1(g_n g_{n+1} + g^\dagger_n g^\dagger_{n+1})$ and $J_2(\sigma^y_{2n,u}\sigma^y_{2n+1,u} + \sigma^x_{2n,l}\sigma^x_{2n+1,l}) = 2iJ_2(g^\dagger_n g_{n+1} + g_n g^\dagger_{n+1})$. A possible means of reversing the site-polarities on adjacent sites would be by the application a "π pulse" involving either of these operators. Schemes for exchanging Majorana modes can be developed using such transport and, in principle, given that the system is a ladder, as opposed to a wire, the need for T-junctions can be eliminated.

Translating between the language of qubits hosted by Majorana modes and spin physics is a rather subtle task requiring further study. As discussed in section II C, a direct correspondence exists between isolated Majorana operators and certain spin operators. Care needs to be taken to ensure that the relevant degrees of freedom are not affected by local fields, and hence, environmental effects. Naïvely, this seems possible given that the Jordan-Wigner string is non-local, and at the same time, the final read out could be more accessible than in fermionic systems by the use of spin-sensitive probes such as magnetic cantilevers. Thus, spin systems may afford an interesting laboratory to explore topological phases of matter and the ideas of topological quantum computation.

B. Quench dynamics

The issue of quenching a topological 1D system through different quantum phases is particularly germane for schemes which involve moving bound Majorana modes localized by shifting topologically non-trivial segments [16, 19]. The dynamics associated with a slow quench across a quantum critical point (QCP) has generated considerable recent interest in its own right [40–52], although its application to topological systems is as yet sparse. To recapitulate some of the basic features, quenching typically involves initializing a system in the ground state of a given Hamiltonian and then varying a parameter of the Hamiltonian at a finite rate $1/\tau$ so as to take it across a QCP. The prominent aspect of such a quench is that one ends up with a finite density of defects, or a residual energy (defined below), which scales as a power of $1/\tau$. In d dimensions, the defect density or residual energy obeys the Kibble-Zurek scaling form $1/\tau^{d\nu/(z\nu+1)}$, where ν and z are respectively the correlation length and dynamical critical exponents of the QCP [40–45]. These exponents are defined by the divergence of the correlation length as $|\lambda - \lambda_c|^{-\nu}$ and the relaxation time as $|\lambda - \lambda_c|^{-z\nu}$, respectively, as a parameter λ in the Hamiltonian approaches a critical value λ_c.

Here, we consider quenching for the case extensively discussed in previous sections, namely, the full vortex sector ($s_n = 1$) in the Kitaev ladder which maps directly onto the 1D p-wave superconductor. In this case, in terms of the Majorana fermions, in the momentum basis, theHamiltonian (8) is of the form

$$H(k) = \sum_k \vec{f}^\dagger_k \begin{pmatrix} 2w\cos k + \mu & 2\Delta\sin k \\ 2\Delta\sin k & -2w\cos k - \mu \end{pmatrix} \vec{f}_k, \tag{27}$$

where $\vec{f}_k^\dagger$ denotes the momentum vector $(f_k^\dagger \;\; f_{-k})$. As detailed earlier, the system respects the dispersion $\omega_k = \pm \sqrt{(2w\cos k + \mu)^2 + 4\Delta^2 \sin^2 k}$ and the resultant phases are as shown in Fig. 1. We study two kinds of quenches: (A) between the two possible topologically non-trivial phases I and II in Fig. 1, and (B) between a topologically non-trivial and topologically trivial phase, such as between phases I and III. We assume a linear quench in which one of the parameters of the Hamiltonian, to be specified below, varies in time as $\alpha(t) = w_0 t/\tau$, so as to take the system through the relevant QCP. We quantify the effect of the quench using the residual energy per site, E_r, attained at the final time, defined as

$$E_r = \lim_{t,N\to\infty} \frac{\langle H(t)\rangle_f - E_0}{N|\alpha(t)|}, \tag{28}$$

Here, N denotes the number of sites, $\langle H\rangle_f$ denotes the expectation value of the Hamiltonian in the final state reached, and E_0 is the ground state energy at $t \to \infty$. We will study the dependence of E_r on τ for $\tau \gg 1$; we expect this to vanish in the adiabatic limit $\tau \to \infty$.

For both kinds of quenches, as shown in the dispersions in Fig. 1, the system consists of two bands which are symmetric about the Fermi energy. In the ground state, the band below the Fermi energy is occupied and the one above is unoccupied. Well within one of the phases, the system is gapped. The quench takes the system through a gapless point at a QCP (as described below) and then into another gapped phase. For any given set of k-modes in Eq. (27), the quench couples the two states in the subsystem respecting $f_k^\dagger f_k + f_{-k}^\dagger f_{-k} = 1$. Thus, the relevant sector contributing to the quench dynamics comprises of the states having occupation numbers $|n_k, n_{-k}\rangle$ equal to $|1,0\rangle$ and $|0,1\rangle$. In this basis, the quenches for cases (A) and (B) take the form

$$\begin{aligned} \mathcal{H}_{Ak}(t) &= (2w_0 \cos k + \mu_0)\, \tau^z \;+\; \alpha(t)(2\sin k)\, \tau^x, \\ \mathcal{H}_{Bk}(t) &= (2w_0 \cos k + \alpha(t))\, \tau^z \;+\; \Delta_0(2\sin k)\, \tau^x, \end{aligned} \tag{29}$$

where w_0, μ_0 and Δ_0 correspond to some fixed parameter values, and τ^a denote the Pauli matrices. Thus, case (A) involves tuning through $\Delta = 0$ for fixed $|\mu_0/(2w_0)| < 1$ and case (B) through $\mu = 2w_0$ for fixed Δ_0/w_0. These take the system through a gapless point which lies at wave vectors $k_c = \pm\cos^{-1}[-\mu_0/(2w_0)]$ in case (A) and $k_c = 0$ and π in case (B). In both cases, the critical exponents are given by $z = \nu = 1$, since the gap is (i) linear in $|k - k_c|$ at the QCP $\alpha = 0$, and (ii) linear in $|\alpha|$ when α is close to zero, for $k = k_c$.

For the linear quench $\alpha(t) = w_0 t/\tau$, the dynamics in both cases maps exactly to the well-known Landau-Zener problem, as with a host of other quenches [41–48, 53]. In particular, for case (B), the probability p_k of ending in an excited state at time $t \gg \tau$ and the net residual energy, for which each sub-system contributes $4p_k$, are given by

$$p_k = \exp[-\pi(2\Delta_0 \sin k)^2 \tau/w_0], \quad \text{and} \quad E_r = \int_0^\pi \frac{dk}{2\pi}\, 4p_k. \tag{30}$$

The probability p_k is largest for the low-energy modes near $k_c = 0$ and π where the gap vanishes at the QCP. In the limit $\tau \gg w_0/\Delta_0^2$, the residual energy is dominated by these modes; expanding around k_c gives a Gaussian integral and the power-law form $E_r \sim 1/\tau^{1/2}$ which is consistent with the Kibble-Zurek power $d\nu/(z\nu+1)$ given that $d = z = \nu = 1$. The same power-law is obtained for case (A), although the expression for the excitation probability p_k looks a bit different from case (B).

In principle, quenching can be studied in the other vortex sectors discussed above. For most sectors, the problem becomes analytically intractable even for a case in which $\Delta = 0$ and only μ is varied in time linearly. As shown by two of us in previous work [54], an interesting situation arises when a pattern of s_n is endowed with a higher symmetry in that some matrix elements of the Hamiltonian in equation (11) are equal to zero. For instance, in the sector in which the signs of s_n form the period 4 pattern $(++--)$, we find that the low-energy modes at $k = 0$ and π (which dominate the generation of residual energy) are coupled via a single intermediate high-energy state lying at $k = -\pi/2$ and $\pi/2$. Using second order perturbation theory to eliminate the high-energy states, we find that the effective time-dependent Hamiltonian governing the low-energy states is given by

$$H_{eff} = \begin{pmatrix} ct^2/\tau^2 & 2k \\ 2k & -ct^2/\tau^2 \end{pmatrix}, \tag{31}$$

where the variable k has been redefined to lie close to 0, and c is a constant. Using a scaling analysis, one can then show that the residual energy goes as $E_r \sim 1/\tau^{2/3}$ [54]. Further work would involve studying such anomalous scaling for quenches into topologically non-trivial phases involving $\Delta \neq 0$.

More generally, if the most relevant states participating in the quench are not directly coupled, but instead are coupled via q intermediate steps, it can be argued that the residual energy, for a linear quench, scales as $E_r \sim 1/\tau^{(q+1)/(q+2)}$. Thus, the quench dynamics in these sectors is also controlled by the QCP, resulting in a power-law scaling of the relevant quantities with respect to the quench rate.

VI. APPLICATIONS TO THE 1D p-WAVE SUPERCONDUCTOR

Given that most of our analysis of the Kitaev ladder involves mapping to the 1D p-wave superconductor, several of our results can be directly applied to the latter system and related ones.

(i) *Periodic potentials and topologically non-trivial phases:-* One of our main results is that vortex patterns in the Kitaev model can alter the topology of the system. The cases that we considered involved periodic patterns in the signs s_n. The primary effect of a periodic pattern is to introduce more bands in momentum space, an effect which can equally well be achieved by the presence of a superlattice or a periodic externally applied potential. Thus, we predict that in the p-wave superconducting system, an alternate means of changing the topological nature of a wire and the associated Majorana end modes is the application a periodic potential. We have developed a straightforward technique for identifying these features even for complex dispersions based on a topological invariant directly derived from equations of motion. Our analysis provides detailed results for the topologically non-trivial phases and isolated Majorana modes in the special case of the external potential controlling only the sign of the local chemical potential on each site. Our results show that such a potential can alter the physics in qualitative ways, for instance, in the case of an alternating site potential, enabling the superconducting gap function to act as a tuning parameter for achieving topologically non-trivial phases.

(ii) *Quench dynamics:-* The quench analysis above provides a word of caution for schemes which entail dynamically changing the topological nature of wire segments. In the thermodynamic limit, our analysis shows that no matter how slowly the system is tuned from one phase to another, the presence of the QCP results in defects whose density has a $1/\tau^{1/2}$ power-law dependence on the tuning rate $1/\tau$. Thus, except in the extreme adiabatic limit, the quench is bound to generate defects which could cause quantum decoherence. Even in the case of changing a finite segment from a topologically non-trivial to a topologically trivial region, it should be kept in mind that the eigenstates of the initial system span its entire length and a local change, particularly involving a gapless point, could affect the entire system and produce a finite density of defects. In fact, the route to equilibrium upon quenching a finite region is in itself an interesting problem which could place stringent constraints on proposed dynamical schemes.

VII. CONCLUSIONS

In conclusion, we have introduced and analyzed a ladder version of Kitaev's honeycomb model. By employing a mapping to a 1D p-wave superconducting system, we have borrowed from the insights provided by this system in terms of topological features. We find an intimate connection between spontaneous symmetry breaking and isolated Majorana modes; this connection provides us with an alternative view of topological order and offers an attractive avenue for the investigation of a wide class of spin systems.

We have performed a detailed study of the ladder system in the presence of vortex arrays and shown that the presence of vortices can dramatically alter the topological properties of the system. We have identified various conditions and configurations of vortices that result in the isolation of Majorana modes, states which are currently being considered as prime candidates for the building blocks in topological quantum computation. We have instigated the study of quench dynamics across quantum critical points in these topological systems, discussing the power-law scaling of the residual energy density; we believe that this avenue unveils important physics from the perspective of non-equilibrium quantum critical phenomena as well as in realistic treatments of the dynamic manipulation of topological entities in quantum computational schemes.

Our findings are germane to various physical systems that are currently under study for their topological properties. Several of our results are directly applicable to quantum wires which, by various methods, can effectively host proximity induced superconducting order [16–19, 23, 25–29, 31]. In the past years, several proposals have focused on realizing the Kitaev honeycomb system in cold atoms trapped in an optical lattice [55, 56]; our results can be immediately translated to these systems. Furthermore, our studies show that it is possible to build a dictionary between topological aspects of non-interacting fermionic systems and ordering in spin systems; an extensive dictionary would enable us to apply insights found in one physical system to the other.

Acknowledgments

This work is supported by the National Science Foundation under the grant DMR 0644022-CAR (W.D. and S.V.) and DST, India under Project No. SR/S2/CMP-27/2006 (D.S.). We would like to thank T. Hughes for detailed and illuminating discussions and D. Ferguson and J. Slingerland for their perceptive comments.

References

[1] A. Kitaev, Ann. Phys. (NY) **321**, 2 (2006).
[2] X.-Y. Feng, G.-M. Zhang, and T. Xiang, Phys. Rev. Lett. **98**, 087204 (2007).
[3] H.-D. Chen and J. Hu, Phys. Rev. B **76**, 193101 (2007).
[4] G. Baskaran, S. Mandal, and R. Shankar, Phys. Rev. Lett. **98**, 247201 (2007).
[5] D.-H. Lee, G.-M. Zhang, and T. Xiang, Phys. Rev. Lett. **99**, 196805 (2007).
[6] H. Yao and S. A. Kivelson, Phys. Rev. Lett. **99**, 247203 (2007).
[7] H.-D. Chen and Z. Nussinov, J. Phys. A **41**, 075001 (2008).
[8] Z. Nussinov and G. Ortiz, Phys. Rev. B **77**, 064302 (2008).
[9] K. P. Schmidt, S. Dusuel, and J. Vidal, Phys. Rev. Lett. **100**, 057208 (2008).
[10] A. Kitaev, arXiv:cond-mat/0010440 (2000).
[11] J. C. Y. Teo and C. L. Kane, Phys. Rev. B **82**, 115120 (2010).
[12] C. Nayak, S. H. Simon, A. Stern, M. Freedman, and S. Das Sarma, Rev. Mod. Phys. **80**, 1083 (2008).
[13] D. A. Ivanov, Phys. Rev. Lett. **86**, 268 (2001).
[14] M. Stone and S.-B. Chung, Phys. Rev. B **73**, 014505 (2006).
[15] G. Kells, A. T. Bolukbasi, V. Lahtinen, J. K. Slingerland, J. K. Pachos, and J. Vala, Phys. Rev. Lett. **101**, 240404 (2008).
[16] J. D. Sau, S. Tewari, and S. Das Sarma, Phys. Rev. A **82**, 052322 (2010).
[17] J. D. Sau, S. Tewari, R. Lutchyn, T. Stanescu, and S. Das Sarma, Phys. Rev. B **82**, 214509 (2010).
[18] Y. Oreg, G. Refael, F. von Oppen, arXiv:1003.1145 (2010).
[19] J. Alicea, Y. Oreg, G. Refael, F. von Oppen, and M. P. A. Fisher, arXiv:1006.4395 (2010).
[20] V. Shivamoggi, G. Refael, and J. E. Moore, arXiv:1004.4585 (2010).
[21] G. Kells, J. Kailasvuori, J. Slingerland, and J. Vala, arXiv:1012.5276 (2010).
[22] M. Z. Hasan and C. L. Kane, arXiv:1002.3895 (2010).
[23] T. Neupert, S. Onoda, and A. Furusaki, arXiv:1008.0849 (2010).
[24] A. R. Akhmerov, J.P. Dahlhaus, F. Hassler, M. Wimmer, and C. W. J. Beenakker, arXiv:1009.5542 (2010).
[25] L. Mao, J. Shi, Q. Niu, and C. Zhang, arXiv:1010.0932 (2010).
[26] M. Duckheim and P. W. Brouwer, arXiv:1011.5839 (2010).
[27] A. C. Potter and P. A. Lee, arXiv:1011.6371 (2010), and Phys. Rev. Lett. **105**, 227003 (2010).
[28] S. B. Chung, H.-J. Zhang, X.-L. Qi, and S.-C. Zhang, arXiv:1011.6422 (2010).
[29] P. Hosur, P. Ghaemi, R. S. K. Mong, and A. Vishwanath, arXiv:1012.0330 (2010).
[30] P. A. Ioselevich and M. V. Feigel'man, arXiv:1012.0407 (2010).
[31] S. Gangadharaiah, B. Braunecker, P. Simon, and D. Loss, arXiv:1101.0094 (2011).
[32] X.-G. Wen and A. Zee, Nucl. Phys. B **316**, 641 (1989).
[33] E. Lieb, T. Schultz, and D. Mattis, Ann. Phys. (NY) **16**, 407 (1961).
[34] E. Barouch, B. M. McCoy, and M. Dresden, Phys. Rev. A **2**, 1075 (1970); E. Barouch and B. M. McCoy, Phys. Rev. A **3**, 786 (1971).
[35] J. E. Bunder and R. H. McKenzie, Phys. Rev. B **60**, 344 (1999).
[36] J. B. Kogut, Rev. Mod. Phys. **51**, 659 (1979).
[37] S. Ostlund and R. Pandit, Phys. Rev. B **29**, 1394 (1984).
[38] D. Sen and S. Lal, Phys. Rev. B **61**, 9001 (2000), and Europhys. Lett. **52**, 337 (2000).
[39] R. Jackiw and C. Rebbi, Phys. Rev. D **13**, 3398 (1976).
[40] T. W. B. Kibble, J. Phys. A, **9**, 1387 (1976), and Phys. Rep. **67**, 183 (1980).
[41] W. H. Zurek, Nature (London), **317**, 505 (1985), and Phys. Rep. **276**, 177 (1996).
[42] W. H. Zurek, U. Dorner and P. Zoller, Phys. Rev. Lett. **95**, 105701 (2005).
[43] J. Dziarmaga, Phys. Rev. Lett. **95**, 245701 (2005).
[44] B. Damski, Phys. Rev. Lett., **95** (2005) 035701.
[45] A. Polkovnikov, Phys. Rev. B **72**, 161201(R) (2005); A. Polkovnikov and V. Gritsev, Nature Phys. **4**, 477 (2008).
[46] R. W. Cherng and L. S. Levitov, Phys. Rev. A **73**, 043614 (2006).
[47] V. Mukherjee, U. Divakaran, A. Dutta, and D. Sen, Phys. Rev. B **76**, 174303 (2007); U. Divakaran, A. Dutta, and D. Sen, Phys. Rev. B **78**, 144301 (2008); U. Divakaran, V. Mukherjee, A. Dutta, and D. Sen, J. Stat. Mech: Theory Exp. P02007 (2009).
[48] S. Deng, G. Ortiz, and L. Viola, EPL **84**, 67008 (2008).
[49] K. Sengupta, D. Sen, and S. Mondal, Phys. Rev. Lett. **100**, 077204 (2008); S. Mondal, D. Sen, and K. Sengupta, Phys. Rev. B **78**, 045101 (2008); D. Sen, K. Sengupta, and S. Mondal, Phys. Rev. Lett. **101**, 016806 (2008); S. Mondal, K. Sengupta, and D. Sen, Phys. Rev. B **79**, 045128 (2009).
[50] R. Barankov and A. Polkovnikov, Phys. Rev. Lett. **101**, 076801 (2008); C. De Grandi, V. Gritsev, and A. Polkovnikov, Phys. Rev. B **81**, 012303 (2010).
[51] J. Dziarmaga, Advances in Physics **59**, 1063 (2010).

[52] A. Dutta, U. Divakaran, D. Sen, B. K. Chakrabarti, T. F. Rosenbaum, and G. Aeppli, arXiv:1012.0653 (2010).
[53] C. Zener, Proc. Roy. Soc. London, Ser. A **137**, 696 (1932); L. Landau and E. M. Lifshitz, *Quantum Mechanics: Non-relativistic Theory*, 2nd Ed. (Pergamon Press, Oxford, 1965).
[54] D. Sen and S. Vishveshwara, EPL **91**, 66009 (2010).
[55] C. Zhang, V. W. Scarola, S. Tewari, and S. Das Sarma, Proc. Natl. Acad. Sci. USA **104**, 18415 (2007).
[56] Y.-J. Han, R. Raussendorf, and L.-M. Duan, Phys. Rev. Lett. **98**, 150404 (2007).